Stability of gravity-capillary solitary waves on shallow water based on the fifth-order Kadomtsev-Petviashvili equation

Yeunwoo Cho*

Department of Mechanical Engineering, Korea Advanced Institute of Science and Technology, 291 Daehak-ro, Yuseong-gu, Daejeon 34141, Republic of Korea

(Received 22 April 2018; revised manuscript received 4 June 2018; published 23 July 2018)

Longitudinal and transverse instabilities of gravity-capillary solitary waves on shallow water are investigated based on the numerical analysis of the fifth-order Kadomtsev-Petviashvili (KP) equation, which describes the wave phenomena on shallow water where the relevant Bond number is less than and close to 1/3. Two-dimensional (2D) depression gravity-capillary solitary waves are stable to longitudinal perturbations. 2D elevation gravity-capillary solitary waves are unstable to longitudinal perturbations and finally evolve into 2D depression gravity-capillary solitary waves. Three-dimensional (3D) finite-amplitude depression gravity-capillary solitary waves are stable to longitudinal perturbations. 3D finite-amplitude elevation gravity-capillary solitary waves are unstable to longitudinal perturbations and finally evolve into an oscillatory state between two different 3D finite-amplitude depression gravity-capillary solitary waves. 3D small-amplitude depression and elevation gravity-capillary solitary waves are unstable to dilation-type longitudinal perturbations and eventually evolve into an oscillatory state between two different 3D finite-amplitude depression gravity-capillary solitary waves. 3D small-amplitude depression and elevation gravity-capillary solitary waves are unstable to contraction-type longitudinal perturbations and eventually become dispersed out toward still water surface. Finally, 2D depression and elevation gravity-capillary solitary waves are unstable to transverse perturbations and eventually evolve into 3D finite-amplitude depression gravity-capillary solitary waves. Therefore, the only stable gravity-capillary solitary waves on shallow water are 3D finite-amplitude depression gravity-capillary solitary waves. In particular, based on the linear stability analysis, a theoretical proof is presented for the long-wave transverse instability of 2D depression and elevation gravity-capillary solitary waves on shallow water.

DOI: 10.1103/PhysRevE.98.012213

I. INTRODUCTION

When both the gravity and the surface tension are equally important in water of a certain depth (h), the phase speed of a linear gravity-capillary wave shows two different behaviors depending on the values of the relevant Bond number ($B = T/\rho g h^2$), where g is the gravitational acceleration, T the surface tension coefficient between air and water, and ρ the density of water. When the Bond number is larger than 1/3 ($B > 1/3$), the phase speed features its minimum at zero wave number and, with a phase speed below its minimum, the Korteweg–de Vries (KdV) -type two-dimensional (2D) and the Kadomtsev-Petviashvili (KP) -type three-dimensional (3D) lump solitary waves can exist, which have been studied extensively [1–5]. The KdV- and KP-type gravity-capillary solitary waves are depression waves whose centers are depressed relative to the still water surface. On the other hand, when the Bond number is less than 1/3 ($B < 1/3$), the phase speed features its minimum at a nonzero wave number and, with a phase speed below its minimum, wave-packet-type 2D and 3D gravity-capillary solitary waves can exist. If the Bond number is zero at finite water depth, i.e., if the surface tension is neglected (pure gravity waves), the phase-speed maximum occurs at a zero wave number. Compared to the case when $B > 1/3$, two kinds of gravity-capillary solitary waves can theoretically exist when $B < 1/3$; elevation and depression-type gravity-capillary solitary waves whose centers are elevated and depressed, respectively, compared to the still water surface [3,5–7]. Under the influence of a longitudinal perturbation, 2D depression gravity-capillary solitary waves are stable while 2D elevation gravity-capillary solitary waves are unstable on shallow water ($B \approx 1/3$ and $B < 1/3$) [8] and deep water ($B \approx 0$) [9,10]. In particular, as a result of a longitudinal instability, 2D elevation gravity-capillary solitary waves on deep water are shown to evolve into 2D depression gravity-capillary solitary waves [9,10]. Similarly, under the influence of a longitudinal perturbation, finite-amplitude 3D depression gravity-capillary solitary waves are stable both on shallow water [11] and on deep water [9,12], whereas finite- and small-amplitude 3D elevation gravity-capillary solitary waves on deep water are unstable and finally evolve into finite-amplitude 3D depression gravity-capillary solitary waves [9,12]; in these two instances, the energy (integral of the wave elevation squared) features a minimum at a critical speed (c_{crit}) near and less than the minimum phase speed (c_{min}) while the maximum depth (wave amplitude) of a gravity-capillary solitary wave increases as the wave-propagation speed becomes farther away from the minimum phase speed (c_{min}). Here, we refer to gravity-capillary solitary waves with $c > c_{\mathrm{crit}}$ as "small-amplitude" gravity-capillary solitary waves with a speed near the minimum phase speed

*Corresponding author: ywoocho@kaist.ac.kr

($c_{\min}$). In the same vein, we refer to gravity-capillary solitary waves with $c < c_{\text{crit}}$ as "finite-amplitude" gravity-capillary solitary waves. Furthermore, under the influence of a dilation-type longitudinal perturbation, small-amplitude 3D depression gravity-capillary solitary waves are unstable and eventually fall into an oscillatory state between two different finite-amplitude 3D depression gravity-capillary solitary waves (focusing-type instability). On the other hand, under the influence of a contraction-type longitudinal perturbation, small-amplitude 3D depression gravity-capillary solitary waves are unstable and will be dispersed out to become a still water surface (defocusing-type instability). These instabilities are identified both on shallow water [11] and on deep water [9,12,13]. Finally, under the influence of a transverse perturbation, 2D depression gravity-capillary solitary waves are proved to be unstable on deep water [9,10,14–16] and on the surface of a finite-depth water [17]. As a result of this transverse instability, 2D depression gravity-capillary solitary waves are shown to finally evolve into 3D finite-amplitude depression gravity-capillary solitary waves on deep water [9,12,16].

As summarized in the aforementioned literature review, most and complete works on the longitudinal instabilities of 2D and 3D gravity-capillary solitary waves and on the transverse instability of 2D gravity-capillary solitary waves have been carried out in deep-water cases. Comparatively, corresponding shallow-water studies are rather sparse. Therefore, the subject of the present paper is on the longitudinal and transverse instabilities of 2D and 3D gravity-capillary solitary waves on shallow water. In the present work, following fifth-order KP equation in terms of the wave elevation $\eta(x, y, t)$ in a normalized form will be studied.

$$\{\eta_t + 3(\eta^2)_x + 2\eta_{xxx} + \eta_{xxxxx}\}_x + \eta_{yy} = 0. \tag{1}$$

Mathematically, Eq. (1) can be interpreted as the modified conventional third-order KP equation with an additional fifth derivative term. A rigorous derivation can be found in [18] and a heuristic derivation based on the dispersion relation is shown in the Appendix. The replacement of $\partial/\partial t$ with $-i\omega$, $\partial/\partial x$ with ik, and $\partial/\partial y$ with il in the linear parts in Eq. (1) results in the following dispersion relation and the phase speed.

$$\omega = -2k^3 + k^5 + \frac{l^2}{k}, \tag{2}$$

$$c_p = \frac{\omega}{k} = -2k^2 + k^4 + \frac{l^2}{k^2}, \tag{3}$$

where k is the wave number in the main wave-propagation direction (say, x), and l the wave number in the correspondingly transverse direction (say, y). Then, the minimum of the phase speed $c_{\min} = -1$ occurs at $(k, l) = (1, 0)$ and $\omega = -1$. A solitary wave exists when $c < c_{\min}$. In the frame of reference moving with a speed $c(x' = x - ct)$, Eq. (1) is rewritten as, by dropping primes,

$$\{\eta_t - c\eta_x + 3(\eta^2)_x + 2\eta_{xxx} + \eta_{xxxxx}\}_x + \eta_{yy} = 0. \tag{4}$$

For a steady-state solitary wave with a certain propagation speed $c < c_{\min}$, one drops the time-dependent term in Eq. (4). For corresponding 2D unsteady and steady solitary waves, one ignores the y-dependent term in Eq. (4). In the following Sec. II, numerical methods solving 2D and 3D, unsteady and steady Eq. (4) are described. Section III is on the longitudinal instabilities of 2D and 3D gravity-capillary solitary waves on shallow water. As mentioned above, the relevant theoretical proofs for the longitudinal instabilities based on the fifth-order KP equation were already given by Calvo *et al.* [8] for 2D gravity-capillary solitary waves and Akylas and Cho [11] for 3D gravity-capillary solitary waves. Therefore, our focus will be on the numerical validation of those results based on the direct numerical simulations of the fifth-order KP equation [Eq. (4)]. Section IV is on the transverse instability of 2D gravity-capillary solitary waves on shallow water.

II. NUMERICAL METHODS

A. Steady solitary-wave solutions

By taking the spatial Fourier transform of Eq. (4) without the time-dependent term,

$$\hat{\eta} = \frac{3}{\{c + 2k^2 - k^4 - (l/k)^2\}}\text{FT}\{\eta^2\} \equiv D(k, l)\text{FT}\{\eta^2\}, \tag{5}$$

where $\text{FT}\{\cdot\}$ denotes the spatial Fourier transform. Equation (5) is solved by the modified Petviashvili method using a simple stabilizing factor in the spatial frequency domain [19]. For the iteration procedure, the initial guess would be $D(k, l)$ in Eq. (5) or any guessed function whose shape is expected to resemble the final solitary-wave solution. The initial guess $D(k, l)$ leads to the primary solitary-wave solution to Eq. (5). In the present case, the primary solitary-wave solution is a depression gravity-capillary solitary wave. If the initial guess is taken as the superposition of depression gravity-capillary solitary-wave solutions with an appropriate relative spacing between each other, the resulting solitary-wave solution is an elevation gravity-capillary solitary wave. In real computations, the Fast Fourier transform (FFT) is used, thus periodic boundary conditions are implied, and the iteration is repeated until the error between each iteration step is less than 10^{-10}. Sufficiently large domain size with $\Delta x = 0.37$ and $\Delta y = 0.29$ is used such that the resultant solitary-wave solutions are locally confined (Fig. 1, Figs. 3 –5, and Fig. 14).

B. Unsteady solitary-wave solutions

By taking the spatial Fourier transform of Eq. (4),

$$\hat{\eta}_t = ik\left(c + 2k^2 - k^4 - \frac{l^2}{k^2}\right)\hat{\eta} - 3ik\text{FT}\{\hat{\eta}^2\}. \tag{6}$$

To solve Eq. (6) numerically, we adopt the leapfrog time stepping as follows.

$$\frac{\hat{\eta}^{(i+1)} - \hat{\eta}^{(i-1)}}{2\Delta t} = ik\left(c + 2k^2 - k^4 - \frac{l^2}{k^2}\right)\{\theta\hat{\eta}^{(i-1)} + (1 - 2\theta)\hat{\eta}^{(i)} + \theta\hat{\eta}^{(i+1)}\} - 3ik\text{FT}\{\hat{\eta}^{(i)^2}\}, \tag{7}$$

where the superscript means a time step and the parameter θ is set to be 1/3. Then, the Fourier-transformed wave elevation at a discretized time step, $i + 1$, can be obtained from those at previous time steps $i - 1$ and i. In the initial calculation for $\hat{\eta}^{(2)}$, two previous values of $\hat{\eta}^{(0)}$ and $\hat{\eta}^{(1)}$ are required.

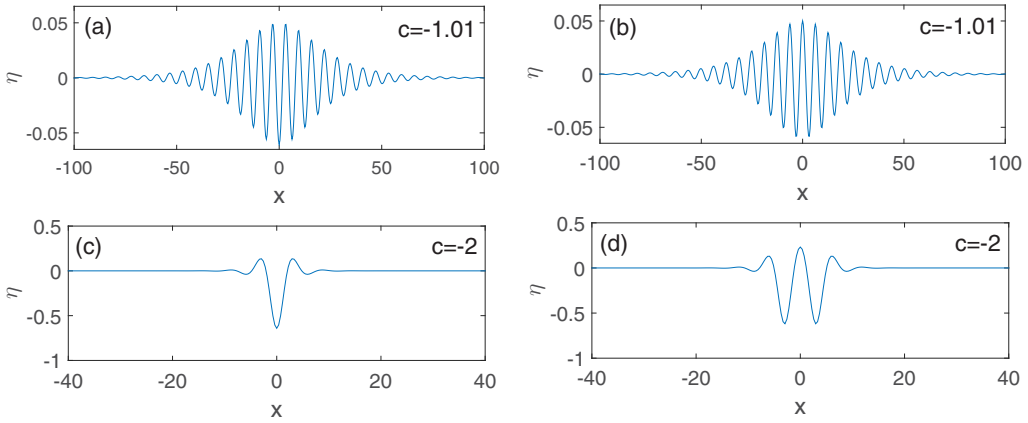

FIG. 1. Two-dimensional gravity-capillary solitary waves with propagation speeds $c = -1.01$ and -2; depression types (left) and elevation types (right).

The value $\hat{\eta}^{(1)}$ is given as the Fourier-transformed value of the perturbed 2D and 3D steady gravity-capillary wave solution. Using the Euler time stepping, Eq. (4) can be discretized as follows.

$$\frac{\hat{\eta}^{(i)} - \hat{\eta}^{(i-1)}}{\Delta t} = ik\left(c + 2k^2 - k^4 - \frac{l^2}{k^2}\right)\hat{\eta}^{(i)} - 3ik\mathrm{FT}\{\hat{\eta}^{(i)^2}\}. \tag{8}$$

Then, the unknown value $\hat{\eta}^{(0)}$, which is the conceptually previous to $\hat{\eta}^{(1)}$, is obtained using the fourth-order Runge-Kutta-type predictor-corrector scheme. In real computation, the time step $\Delta t = 0.001$ with spatial resolutions of $\Delta x = 0.37$ and $\Delta y = 0.29$ is used for a stable computation for a long time ($\sim t = 800$). Also, sufficiently large domain size is used such that reflections from the boundaries are minimized (Fig. 2, Figs. 6 –13, Fig. 15, and Fig. 16).

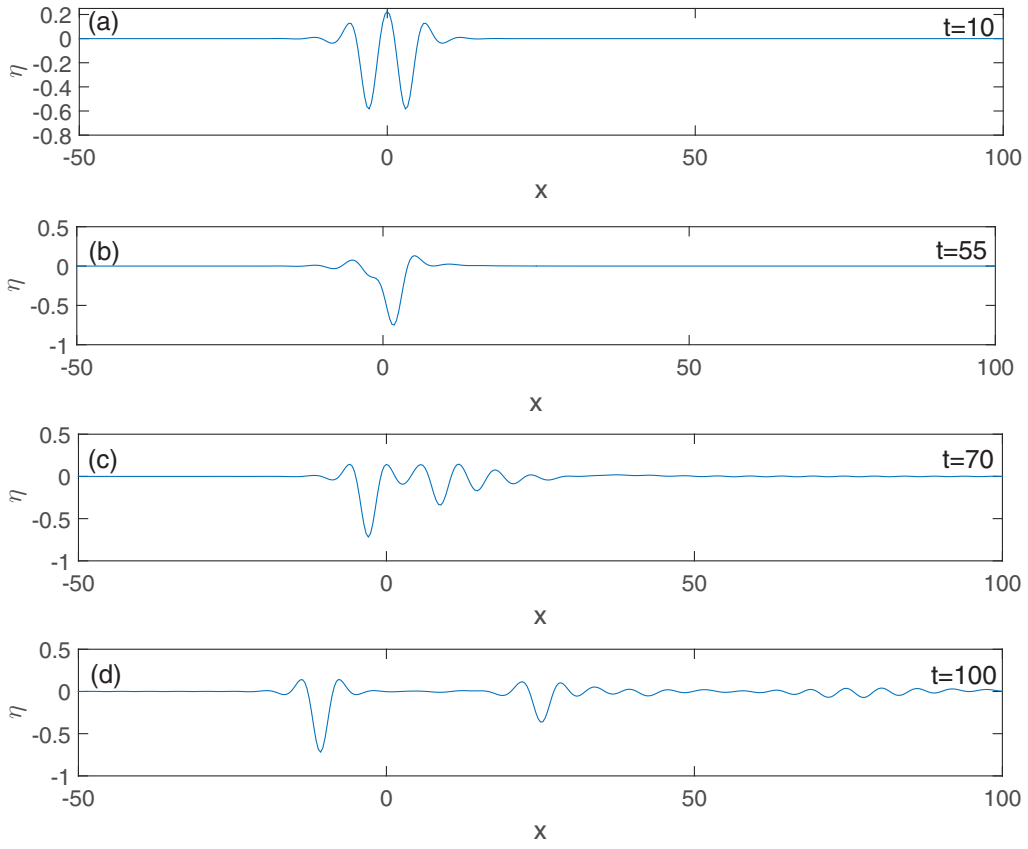

FIG. 2. Evolution of the initial two-dimensional elevation solitary wave with $c = -2$ in the frame of reference moving with speeds $c = -2$.

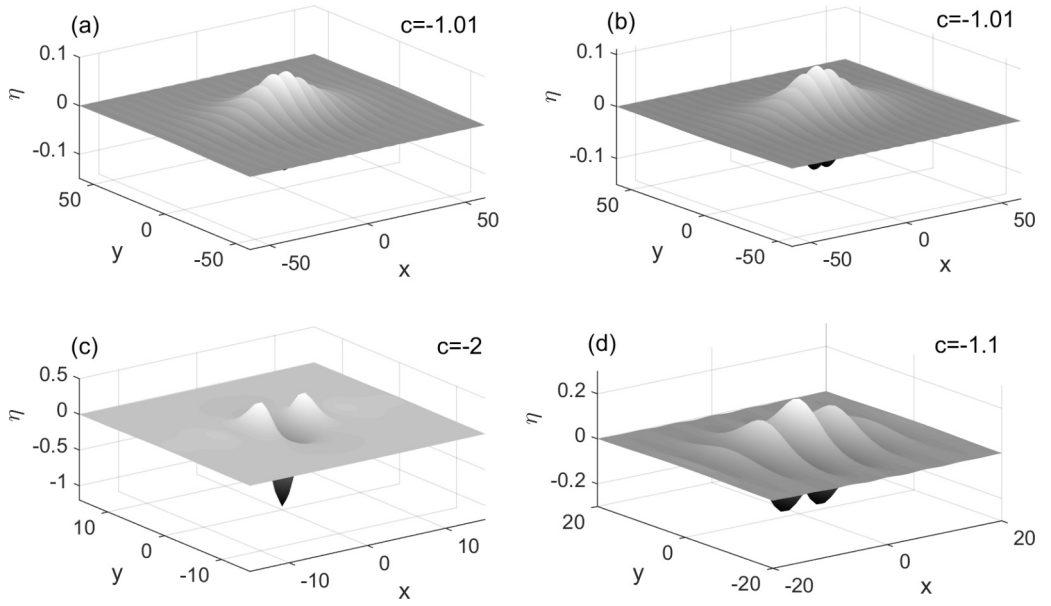

FIG. 3. Three-dimensional gravity-capillary solitary waves. Left: depression types ($c = -1.01$ and -2). Right: elevation types ($c = -1.01$ and -1.1).

III. LONGITUDINAL INSTABILITIES OF 2D AND 3D GRAVITY-CAPILLARY SOLITARY WAVES ON SHALLOW WATER

A. Longitudinal instability of 2D gravity-capillary solitary waves on shallow water

For a given wave-propagation speed c, steady-state 2D depression and elevation gravity-capillary solitary-wave solutions can be obtained by solving Eq. (4) without time-dependent and y-dependent terms, using the modified Petviashvili method [19] described in Sec. II. Figure 1 shows representative 2D depression and elevation gravity-capillary solitary-wave solutions for wave-propagation speeds $c = -1.01$ and -2. Very close to the minimum phase speed, $c_{\min} = -1$, 2D depression and elevation gravity-capillary solitary waves are wave-packet types. As the magnitude of c increases, the 2D depression and elevation gravity-capillary solitary wave becomes more locally confined and its maximum depth increases. Although both depression- and elevation-type steady 2D gravity-capillary solitary waves are possible, depression waves are stable and elevation waves are unstable to longitudinal perturbations, which is theoretically proved by Calvo *et al.* [8]. By assuming the solution to 2D Eq. (4) to be decomposed as

$$\begin{aligned} \eta(x,t) &= \bar{\eta}(x) + \eta'(x,t) = \bar{\eta}(x) + \hat{\eta}(x)e^{\lambda t}; \\ \hat{\eta} &\to 0 \quad (x \to \pm\infty), \end{aligned} \tag{9}$$

where $\bar{\eta}$ is a steady 2D depression and elevation gravity-capillary solitary wave and $\eta'(x,t)$ is the perturbation term. Then, the following eigenvalue problem is derived.

$$\lambda\hat{\eta} - c\hat{\eta}_x + 6(\bar{\eta}\hat{\eta})_x + 2\hat{\eta}_{xxx} + \hat{\eta}_{xxxxx} = 0. \tag{10}$$

By solving Eq. (10) numerically, they show that real parts of the associated eigenvalues (growth rate: λ) are negative and positive, respectively, for 2D depression and elevation gravity-capillary solitary waves and thus prove that 2D depression and elevation gravity-capillary solitary waves are, respectively, longitudinally stable and unstable. In addition, they perform an asymptotic analysis by introducing the following expansion.

$$\hat{\eta} = \hat{\eta}^{(0)} + \lambda\hat{\eta}^{(1)} + \lambda^2\hat{\eta}^{(0)} + \cdots; \quad |\lambda| \ll 1. \tag{11}$$

By substituting Eq. (11) into Eq. (10), they theoretically show that 2D elevation gravity-capillary solitary waves are unstable with a positive growth rate λ. On the other hand, no instability is predicted for 2D depression gravity-capillary solitary waves at least to leading order in the asymptotic analysis. We solve the 2D unsteady evolution equation with an initial condition of a longitudinally perturbed 2D depression or elevation gravity-capillary solitary wave. Equivalently, we solve the 2D unsteady evolution equation with an initial condition of the unperturbed 2D depression or elevation gravity-capillary solitary wave for a sufficiently long time such that the accumulated numerical error plays as a longitudinal perturbation. 2D depression gravity-capillary solitary waves in Fig. 1 maintain their shapes during long-time simulations whether there are initial perturbations or not, and, thus, are stable. On the other hand, 2D elevation gravity-capillary solitary waves turn out to be unstable. For example, Fig. 2 shows a long-time evolution of the initially unperturbed 2D elevation solitary wave with a propagation speed $c = -2$. The onset of the longitudinal instability can be seen at $t = 55$ and, thereafter, the resultant formation of two 2D depression gravity-capillary solitary waves are observed, which propagate stably with their own speeds.

B. Longitudinal instability of 3D gravity-capillary solitary waves on shallow water

Similar to 2D cases, for a given c, steady-state 3D depression and elevation gravity-capillary solitary-wave solutions can be obtained by solving Eq. (4) without the time-dependent term, using the modified Petviashvili method [19] described in Sec. II. Figure 3 shows representative 3D depression gravity-capillary solitary waves with $c = -1.01$ and -2 and

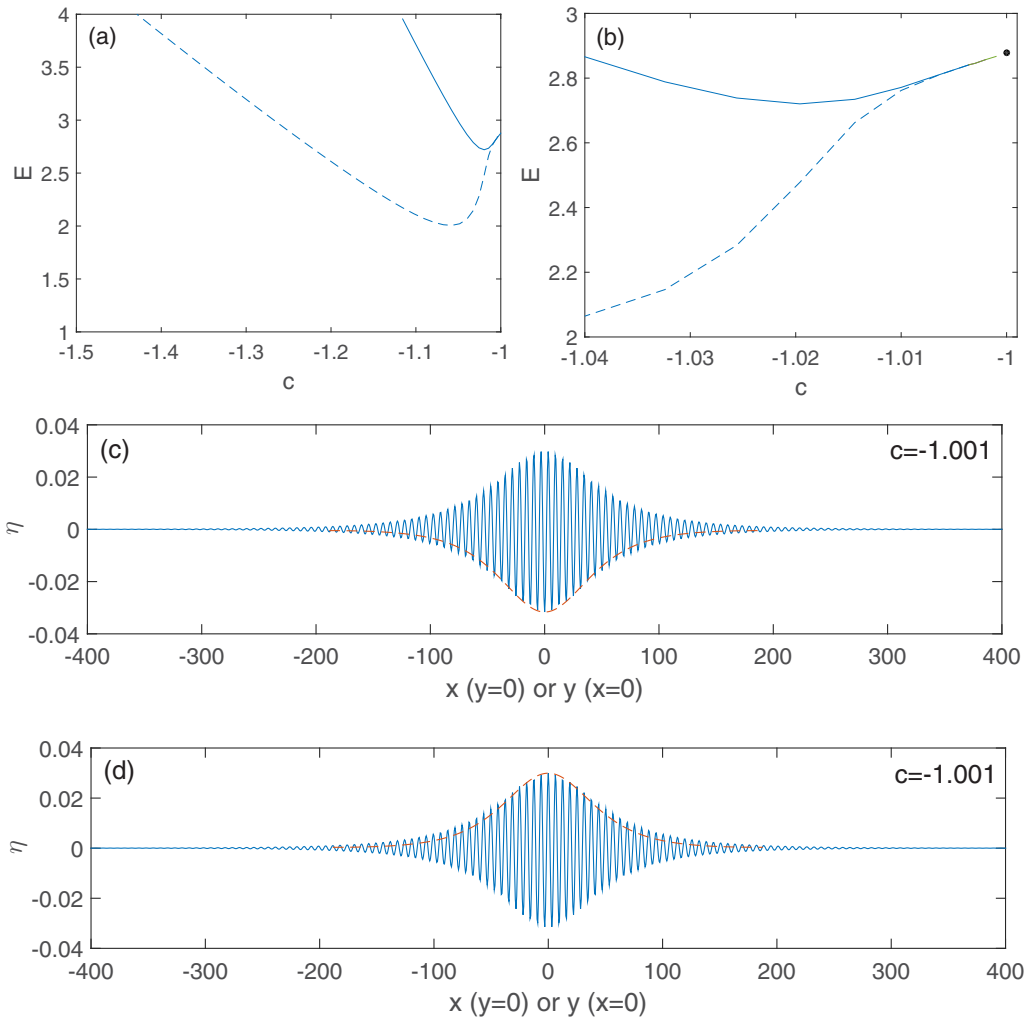

FIG. 4. E-c curves of 3D depression and elevation gravity-capillary solitary waves on shallow water and wave profiles at $c = -1.001$. (a) E-c curves for $-1.5 < c < -1$; (b) magnified E-c curves near $c_{\min} = -1$; and (c),(d) cross-sectional views for $x = 0$ (dashed) and $y = 0$ (solid) of 3D depression (c) and elevation (d) gravity-capillary solitary waves with $c = -1.001$.

elevation solitary waves with $c = -1.01$ and -1.1. Like 2D gravity-capillary solitary waves, very close to the minimum phase speed, $c_{\min} = -1$, 3D depression and elevation gravity-capillary solitary waves are wave-packet types. As the magnitude of c increases, the 3D depression and elevation gravity-capillary solitary wave becomes more locally confined and its maximum depth increases. The stability characteristics of steady 3D elevation and depression gravity-capillary solitary waves are more complex than their 2D counterparts. Compared to the stability analysis for 2D depression and elevation gravity-capillary solitary waves [8], similar stability analysis for 3D depression gravity-capillary solitary waves is performed in Akylas and Cho [11]. By assuming the solution to Eq. (4) to be decomposed as

$$\eta(x, y, t) = \bar{\eta}(x, y) + \eta'(x, y, t) = \bar{\eta}(x, y) + \hat{\eta}(x, y)e^{\lambda t};$$
$$\hat{\eta} \to 0(x^2 + y^2 \to \infty), \tag{12}$$

where $\bar{\eta}$ is a steady 3D depression gravity-capillary solitary wave and $\eta'(x, y, t)$ is a perturbation term. Then, the following

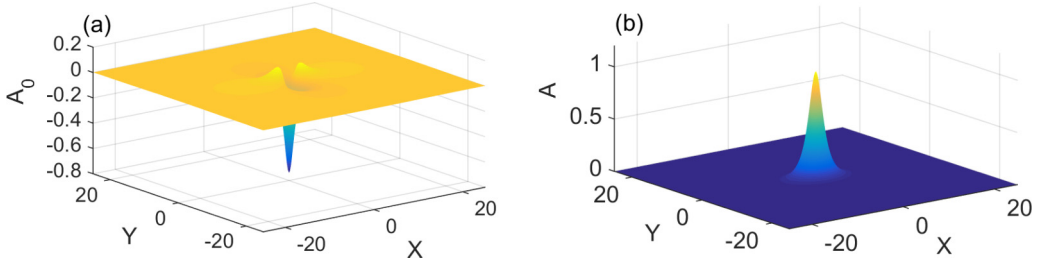

FIG. 5. Numerically computed $A_0(X, Y)$ and $A(X, Y)$ of BRDS equation system [Eqs. (19) and (20)]. (a) $A_0(X, Y)$, (b) $A(X, Y)$.

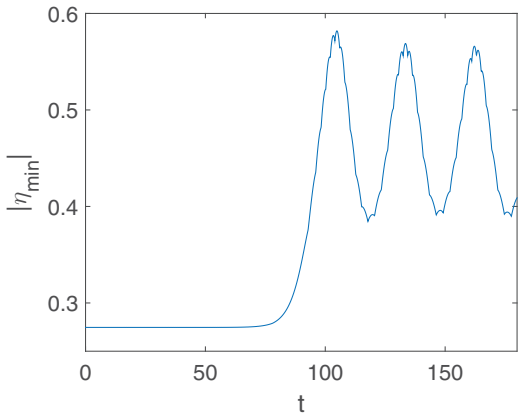

FIG. 6. Time history of the maximum depth of the initially unperturbed finite-amplitude 3D elevation gravity-capillary solitary wave with $c = -1.1$.

eigenvalue problem is derived.

$$\{\lambda\hat{\eta} - c\hat{\eta}_x + 6(\bar{\eta}\hat{\eta})_x + 2\hat{\eta}_{xxx} + \hat{\eta}_{xxxxx}\}_x + \hat{\eta}_{yy} = 0. \quad (13)$$

By solving Eq. (13) numerically, they show that the associated eigenvalue (growth rate: λ) is positive for $-1.053 < c < -1$ for 3D depression gravity-capillary solitary waves. They also show that no instability is detected when $c < -1.09$. This suggests that an exchange of stability takes place for $-1.09 < c < -1.053$. To check this hypothesis, they perform an asymptotic analysis by introducing the following expansion.

$$\hat{\eta} = \hat{\eta}^{(0)} + \lambda\hat{\eta}^{(1)} + \lambda^2\hat{\eta}^{(0)} + \cdots; \quad |\lambda| \ll 1. \quad (14)$$

By substituting Eq. (14) into Eq. (13), it is found that there should be an existence of an energy minimum as a necessary condition for an exchange of stability and it is numerically confirmed that there exists an energy minimum at $c = -1.06$, where the energy of a gravity-capillary solitary wave with a propagation speed c can be defined as follows.

$$E = \int_{-\infty}^{\infty}\int_{-\infty}^{\infty} \eta^2(x, y; c)dx\,dy. \quad (15)$$

The resultant E-c curves of 3D elevation and depression gravity-capillary solitary waves on shallow water are shown in Figs. 4(a) and 4(b) (dashed: depression waves; solid: elevation waves). For readers' information, 3D elevation gravity-capillary solitary waves are not considered in Akylas and Cho [11]. In both cases, there exists a minimum energy E at a critical wave-propagation speed c_{crit} near the minimum phase speed $c_{min} = -1$, i.e.,

$$\left.\frac{\partial E}{\partial c}\right|_{c_{crit} \neq c_{min}} = 0. \quad (16)$$

For depression and elevation waves, the minimum E occurs at $c_{crit} = -1.06$ and $c_{crit} = -1.02$, respectively [Fig. 4(a)]. Figure 4(b) shows the magnified version of Fig. 4(a) near speed $c_{min} = -1$. As c approaches the minimum phase speed $c_{min} = -1$, both energy curves of depression (dashed) and elevation (solid) gravity-capillary solitary waves collapse onto each other. The end point of the collapsed curve represents the energy values, $E = 2.867$, of depression and elevation gravity-capillary solitary waves with a speed $c = -1.001$ [Figs. 4(c) and 4(d)]. The "dot" in Fig. 4(b) represents the energy value, $E = 2.877$, at $c = c_{min} = -1$. This value is numerically computed by solving the so-called Benney-Roskes-Davey-Stewartson equation (BRDS) system [20,21].

The BRDS equation system is derived from the asymptotic analysis of the fifth-order KP equation, Eq. (4), in the small-amplitude weakly nonlinear limit as follows.

$$c = -1 - \varepsilon^2; \quad 0 < \varepsilon \ll 1, \quad (17)$$

$$\eta = \frac{\varepsilon}{2}\{A(X, Y)e^{ix} + \text{c.c.}\} + \varepsilon^2 A_0(X, Y) + \varepsilon^2\{A_2(X, Y)e^{2ix} + \text{c.c.}\} + \cdots, \quad (18)$$

where $X = \varepsilon x$, $Y = \varepsilon y$ are slow envelope variables and c.c. denotes the complex conjugate. By substituting Eqs. (17) and (18) into Eq. (4), then, by collecting zeroth, primary, and

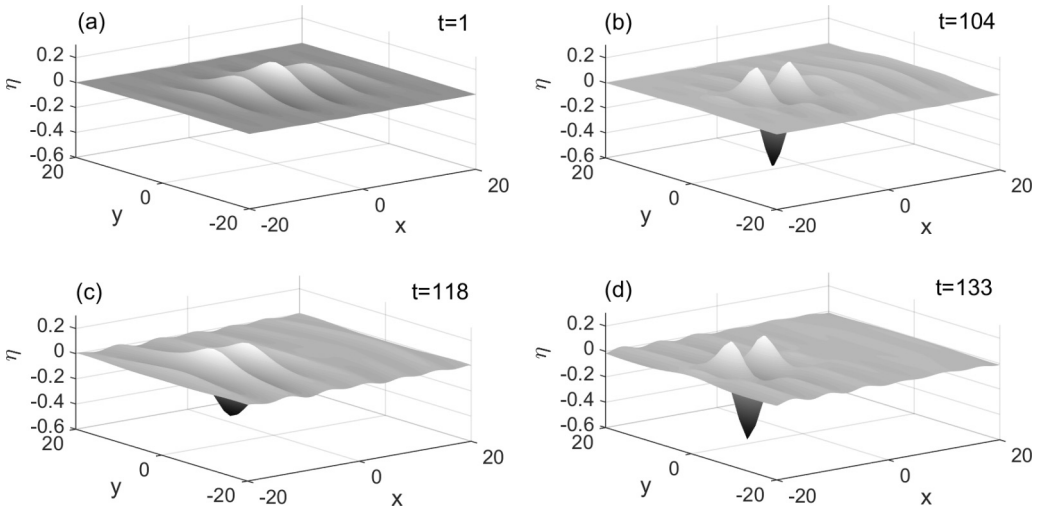

FIG. 7. Evolution of the initially unperturbed finite-amplitude 3D elevation solitary wave with $c = -1.1$ in the frame of reference moving with speeds $c = -1.1$.

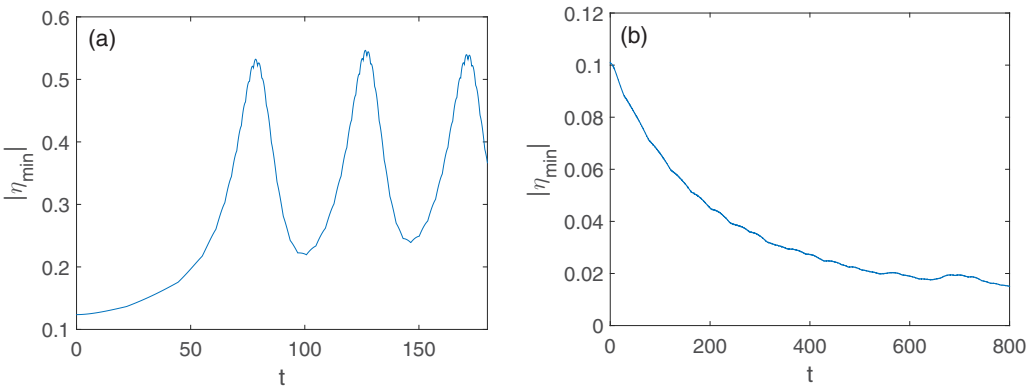

FIG. 8. Time histories of the maximum depth of the initially perturbed 3D small-amplitude depression solitary wave with $c = -1.01$. (a) Initial dilation-type perturbation (10%). (b) Initial contraction-type perturbation (−10%).

secondary harmonic terms, one obtains the following BRDS equation system.

$$A_{0,XX} + A_{0,YY} = -\tfrac{3}{2}(|A|^2)_{XX}, \tag{19}$$

$$-A + 4A_{XX} + A_{YY} + \tfrac{1}{2}A^3 - 6A_0A = 0, \tag{20}$$

$$A_2 = -\tfrac{1}{12}A^2. \tag{21}$$

The BRDS equation system [Eqs. (19) and (20)] is numerically solved by a modified Petviashvili method [19] and the resultant solutions $A_0(X, Y)$ and $A(X, Y)$ are shown in Fig. 5. Then, from Eq. (18), the wave energy E is

$$\begin{aligned} E &= \frac{\varepsilon^2}{4}\int_{-\infty}^{\infty}\int_{-\infty}^{\infty} 2|A|^2 dx\,dy + \varepsilon^4\int_{-\infty}^{\infty}\int_{-\infty}^{\infty} A_0^2 dx\,dy \\ &\quad + \varepsilon^4\int_{-\infty}^{\infty}\int_{-\infty}^{\infty} 2|A_2|^2 dx\,dy + \cdots \\ &= \frac{1}{2}\int_{-\infty}^{\infty}\int_{-\infty}^{\infty} |A|^2 dX\,dY + \varepsilon^2\left(\int_{-\infty}^{\infty}\int_{-\infty}^{\infty} A_0^2 dX\,dY\right. \\ &\quad \left. + \int_{-\infty}^{\infty}\int_{-\infty}^{\infty} \frac{1}{72}|A|^4 dX\,dY\right) + \cdots \\ &= 2.877 + 1.926\varepsilon^2 = 0.951 - 1.926c. \end{aligned} \tag{22}$$

According to Eq. (22), for the end point $(c, E) = (-1.001, 2.867)$ computed from Eq. (4) to be connected with the point $(c_{min}, E) = (-1, 2.877)$, there may be an energy maximum in the extremely narrow region $-1.001 < c < -1$, which, however, is not identified in Fig. 5(b) for the present numerical resolution. In 3D cases, as c decreases the maximum depth or the wave amplitude monotonically increases. Also, considering E-c curves (Fig. 4), we refer to gravity-capillary solitary waves with $c > c_{crit}$ as "small-amplitude" gravity-capillary solitary waves. In the same vein, we refer to gravity-capillary solitary waves with $c < c_{crit}$ as "finite-amplitude" gravity-capillary solitary waves. Small-amplitude and finite-amplitude gravity-capillary solitary waves have different stability characteristics to longitudinal perturbations. In the next sections, it will be numerically shown that finite-amplitude 3D depression gravity-capillary solitary waves are stable, but small-amplitude 3D depression gravity-capillary solitary waves are unstable to longitudinal perturbations. On the other hand, both finite-amplitude and small-amplitude 3D elevation gravity-capillary solitary waves are unstable to longitudinal perturbations. Overall, we solve the unsteady evolution equation, Eq. (4), with an initial condition of a longitudinally perturbed 3-D depression or elevation gravity-capillary solitary wave. Equivalently, we solve Eq. (4) with the initial condition of the unperturbed 3D depression or elevation gravity-capillary solitary wave for sufficiently long time such that the accumulated numerical error plays as a longitudinal perturbation. In solving Eq. (4), spatially, the spectral method is used with $\Delta x = 0.37$ and $\Delta y = 0.29$ and, temporally, the predictor-corrector scheme is used with $\Delta t = 0.001$, as mentioned in Sec. II.

1. Longitudinal instability of 3D finite-amplitude gravity-capillary solitary waves on shallow water

3D finite-amplitude depression gravity-capillary solitary waves ($c < c_{crit} = -1.06$) in Fig. 3 maintain their shapes during long-time simulations under the influence of longitudinal perturbations and, thus, are stable. On the other hand, 3D finite-amplitude elevation gravity-capillary solitary waves ($c < c_{crit} = -1.02$) turn out to be unstable to longitudinal perturbations. For example, Fig. 6 shows the time history of the maximum depth of the initially unperturbed 3D elevation gravity-capillary solitary wave with a propagation speed $c = -1.1$. The onset of a longitudinal instability during the numerical simulation can be seen at about $t = 90$. Figure 7 shows the associated 3D snapshots showing the resultant oscillatory state between two 3D finite-amplitude depression gravity-capillary solitary waves after the onset of instability.

2. Longitudinal instability of 3D small-amplitude gravity-capillary solitary waves on shallow water

Compared to 3D finite-amplitude gravity-capillary solitary waves ($c < c_{crit}$), longitudinal instability characteristics of 3D small-amplitude gravity-capillary solitary waves ($c > c_{crit}$) are

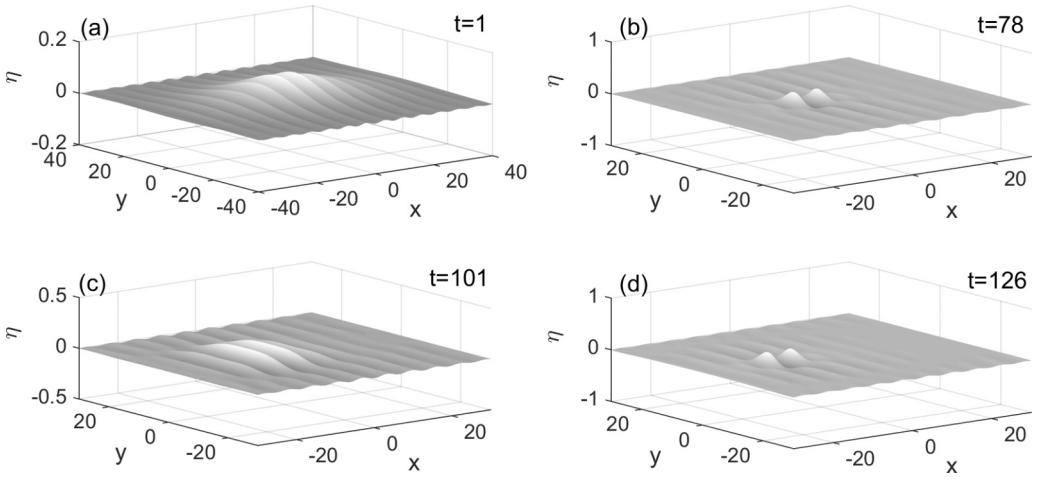

FIG. 9. Evolution of the initially perturbed 3D small-amplitude depression solitary wave with $c = -1.01$, corresponding to the dilation-type perturbation case (10%) in Fig. 8(a).

more delicate depending on the sign of the perturbations. If perturbed initial wave profiles ($c > c_{\text{crit}}$) are expressed as $\eta = (1 + \delta)\bar{\eta}$, where $\bar{\eta}$ is unperturbed 3D small-amplitude depression and elevation gravity-capillary solitary wave profiles, then, under the influence of a dilation-type perturbation ($\delta > 0$) above a certain threshold value δ^+, 3D small-amplitude depression and elevation gravity-capillary solitary waves cannot maintain their wave profiles and each final state will be an oscillatory state between two 3D finite-amplitude depression gravity-capillary solitary waves. Under the influence of a contraction-type perturbation ($\delta < 0$) below a certain threshold δ^-, initial 3D gravity-capillary solitary waves will be dispersed out toward still water. These behaviors are related to the already mentioned BRDS equation system. The BRDS equation system predicts the focusing (finite-time blowup) of the solution if the perturbation is a dilation type and the defocusing (becoming dispersed out to be zero states) of the solution if the perturbation is a contraction type. The focusing and defocusing of the solution of the BRDS equation system are related, respectively, to the oscillatory and zero states (still water) in the fifth-order KP equation. Although related to each other, no finite-time blowup can be seen in the simulation of the fifth-order KP equation. In the present numerical simulation, for $\delta^- = -0.02 < \delta < \delta^+ = 0.02$, initially perturbed waves are stable. For $\delta > \delta^+ = 0.02$, initially perturbed waves become final states where oscillatory states between two 3D finite-amplitude depression gravity-capillary solitary waves. For $\delta < -0.02$, initially perturbed waves become dispersed out toward still water. For example, Figs. 8(a) and 8(b) show the time histories of the maximum depth of the initially perturbed 3D small-amplitude depression gravity-capillary solitary waves with a propagation speed $c = -1.01$ for initial dilation-type (10%) and contraction-type (−10%) perturbations, respectively. In other words, the initial wave profiles are $\eta = 1.1\bar{\eta}$ or $\eta = 0.9\bar{\eta}$, where $\bar{\eta}$ are unperturbed 3D small-amplitude depression gravity-capillary solitary wave profiles with $c = -1.01$. Figures 9 and 10 show the associated 3D snapshots. Corresponding figures for 3D elevation solitary waves with a propagation speed $c = -1.01$ are Figs. 11(a), 11(b), 12, and 13.

IV. TRANSVERSE INSTABILITY OF 2D GRAVITY-CAPILLARY SOLITARY WAVES ON SHALLOW WATER

From the stability results in Sec. III, we see that 2D depression and elevation gravity-capillary solitary waves are stable to longitudinal perturbations. Therefore, in 2D, the remaining question on the stability is the stability of 2D depression and elevation gravity-capillary solitary waves to transverse perturbations. If they are unstable, we expect that 2D depression and elevation gravity-capillary solitary waves will be transformed into 3D finite-amplitude depression gravity-capillary solitary waves, based on the results in Sec. III where it is seen that 3D finite-amplitude depression gravity-capillary solitary waves are stable to longitudinal perturbations. In the next sections A and B, from the linear stability analysis and the associated numerical simulations, respectively, we will show that the 2D depression and elevation gravity-capillary solitary waves are unstable to transverse perturbations. Although the method of the analytical proof may be regarded as standard (e.g., [17]), its application to the fifth-order KP equation is new and is presented here.

A. Linear stability analysis

Let us consider the 3D unsteady evolution equation, Eq. (4), which is written in the frame of reference moving with a speed c in the x direction.

$$\{\eta_t - c\eta_x + 3(\eta^2)_x + 2\eta_{xxx} + \eta_{xxxxx}\}_x + \eta_{yy} = 0. \quad (23)$$

Equation (23) admits both 2D and 3D solitary-wave solutions. The 2D steady-state solitary-wave solution, $\bar{\eta}(x)$, satisfies the following equation.

$$-c\bar{\eta}_x + 3(\bar{\eta}^2)_x + 2\bar{\eta}_{xxx} + \bar{\eta}_{xxxxx} = 0. \quad (24)$$

The transversely perturbed wave solution to Eq. (24) can be written as follows.

$$\eta(x, y, t) = \bar{\eta}(x) + \eta'(x, y, t); \quad |\eta'/\bar{\eta}| \ll 1,$$
$$\eta' = \varphi(x)e^{\lambda t + i\beta y}, \quad \varphi \to 0 \quad (x \to \pm\infty), \quad (25)$$

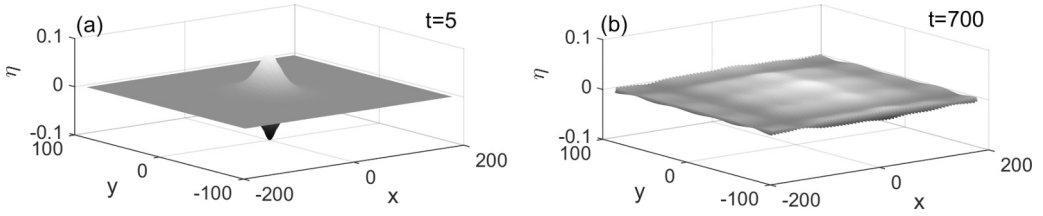

FIG. 10. Evolution of the initially perturbed 3D small-amplitude depression solitary wave with $c = -1.01$, corresponding to the contraction-type perturbation case (-10%) in Fig. 8(b).

where λ is the temporal growth rate and β is the wave number in the transverse direction and the function φ is locally confined. By substituting Eq. (25) into Eq. (23) and by neglecting $O(\eta'^2)$ or $O(\varphi^2)$ and higher,

$$\lambda\varphi_x - c\varphi_{xx} + 6(\bar{\eta}\varphi)_{xx} + 2\varphi_{xxxx} + \varphi_{xxxxxx} - \beta^2\varphi = 0. \tag{26}$$

In the long-wave perturbation limit ($\beta \ll 1$), upon expanding φ and λ in the ascending power of β,

$$\begin{aligned} \varphi &= \varphi^{(0)} + \beta\varphi^{(1)} + \beta^2\varphi^{(2)} + \cdots, \\ \lambda &= \lambda_0 + \beta\lambda_1 + \beta^2\lambda_2 + \cdots, \end{aligned} \tag{27}$$

and substituting Eq. (27) into Eq. (26), one obtains a series of equations according to the order of magnitudes $O(1)$, $O(\beta)$, $O(\beta^2)$, etc.

$$O(1): \; -c\varphi^{(0)}_{xx} + 6(\bar{\eta}\varphi^{(0)})_{xx} + 2\varphi^{(0)}_{4x} + \varphi^{(0)}_{6x} = -\lambda_0\varphi^{(0)}_x;$$
$$\lambda_0 = 0, \quad \varphi^{(0)} = \bar{\eta}_x. \tag{28}$$

$$O(\beta): \; -c\varphi^{(1)}_x + 6(\bar{\eta}\varphi^{(1)})_x + 2\varphi^{(1)}_{xxx} + \varphi^{(1)}_{xxxxx} = -\lambda_1\varphi^{(0)};$$
$$\varphi^{(1)} = -\lambda_1\bar{\eta}_c. \tag{29}$$

$$O(\beta^2): \; -c\varphi^{(2)}_{xx} + 6(\bar{\eta}\varphi^{(2)})_{xx} + 2\varphi^{(2)}_{4x} + \varphi^{(2)}_{6x} = \varphi^{(0)} - \lambda_1\varphi^{(1)}_x - \lambda_2\varphi^{(0)}_x. \tag{30}$$

By substituting Eqs. (28) and (29) into Eq. (30) and, further, by integration with respect to x,

$$\begin{aligned} L\varphi^{(2)} &= \int_x \bar{\eta}\,dx + \lambda_1^2\int_x \bar{\eta}_c\,dx - \lambda_2\bar{\eta}; \\ L &= -c + 6\bar{\eta} + 2\frac{\partial^2}{\partial x^2} + \frac{\partial^4}{\partial x^4}. \end{aligned} \tag{31}$$

The adjoint operator (L^A) to L is L. Then, the relevant homogeneous equation to Eq. (31) is

$$L^A\varphi^{(2)}_h = L\varphi^{(2)}_h = 0; \quad \varphi^{(2)}_h = \bar{\eta}_x. \tag{32}$$

Therefore, from the usual solvability argument, a solution to the homogeneous equation should be orthogonal to the right-hand side in Eq. (31) as follows.

$$\int_{-\infty}^{\infty}\left(\int_x \bar{\eta}\,dx + \lambda_1^2\int_x \bar{\eta}_c\,dx - \lambda_2\bar{\eta}\right)\bar{\eta}_x\,dx = 0. \tag{33}$$

Using the fact that the wave profile ($\bar{\eta}$) and its derivatives are locally confined, Eq. (33) is finally reduced to the following equation for the growth rate λ.

$$\lambda_1^2 = -\frac{\int_{-\infty}^{\infty}\bar{\eta}^2\,dx}{\frac{1}{2}\frac{\partial}{\partial c}\int_{-\infty}^{\infty}\bar{\eta}^2\,dx}. \tag{34}$$

The numerator in Eq. (34) is always positive. Therefore, there is a transverse instability (λ is real) if the following condition satisfies

$$\frac{\partial}{\partial c}\int_{-\infty}^{\infty}\bar{\eta}^2\,dx = \frac{\partial E}{\partial c} < 0. \tag{35}$$

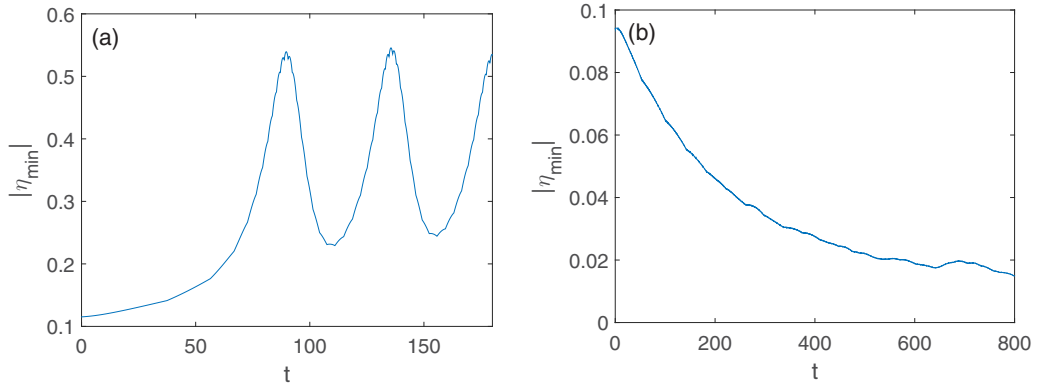

FIG. 11. Time histories of the maximum depth of the initially perturbed 3D small-amplitude elevation solitary wave with $c = -1.01$. (a) Dilation-type perturbation (10%). (b) Contraction-type (-10%) perturbation.

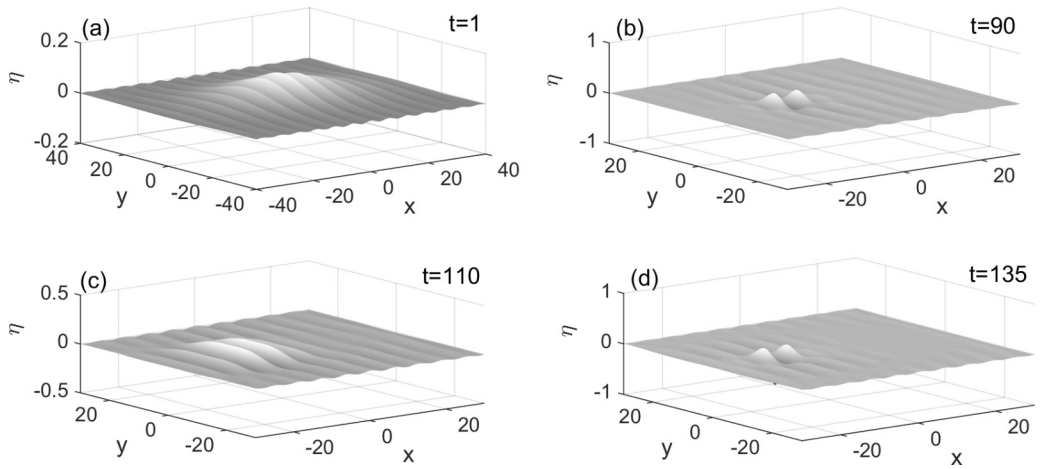

FIG. 12. Evolution of the initially perturbed 3D small-amplitude elevation solitary wave with $c = -1.01$, corresponding to the dilation-type perturbation case (10%) in Fig. 11(a).

Figures14(a) and 14(b) show that Eq. (35) is satisfied both for the 2D depression and elevation gravity-capillary solitary waves. Therefore, 2D depression and elevation gravity-capillary solitary waves are unstable to transverse perturbations.

B. Numerical simulations

In the previous Sec. III A, based on the linear stability analysis, we proved the onset of the instability of 2D depression and elevation gravity-capillary solitary waves under the influence of long-wave transverse perturbations. To understand the associated nonlinear behavior, we perform a transient numerical simulation of transversely perturbed initial 2D depression and elevation gravity-capillary solitary waves with $c = -2$, respectively. In the simulations, the range of the transverse direction is $-6\pi < y < 6\pi$ and the initial conditions are as follows.

$$\eta(x, y, t = 0) = \bar{\eta}(x) + \bar{\eta}_x \cos\left(\frac{y}{12}\right), \tag{36}$$

which has the form of Eq. (28), i.e., $\varphi^{(0)} = \bar{\eta}_x$ and $\beta = 1/12 \ll 1$. In Fig. 15, the transversely perturbed initial 2D depression gravity-capillary solitary wave, which propagates with speed $c = -2$ in the x direction, is finally transformed into two 3D depression gravity-capillary solitary waves propagating in the x direction. In Fig. 16, a transversely perturbed initial 2D elevation gravity-capillary solitary wave, which propagates with speed $c = -2$ in the x direction, is finally transformed into two 3D depression gravity-capillary solitary waves propagating in the x direction and two 3D depression gravity-capillary solitary waves propagating in the oblique directions.

V. SUMMARY AND DISCUSSION

We conducted a comprehensive theoretical and numerical study on the longitudinal and transverse instabilities of 2D and 3D depression and elevation gravity-capillary solitary waves on shallow water based on the fifth-order KP equation which is derived from the condition that the relevant Bond number is less than and close to 1/3. The fifth-order KP equation features its phase speed minimum at a nonzero wave number. Comparatively, if the Bond number is larger than 1/3, the phase speed minimum occurs at a zero wave number and if the Bond number is zero at finite water depth, i.e., if the surface tension is neglected (pure gravity waves), the phase-speed maximum occurs at a zero wave number. While the conventional third-order KP equation (in 2D, KdV) is an integrable equation, the present fifth-order KP equation is a nonintegrable one. Since no exact analytical solutions are known, the present work mainly focuses on the numerical study with regard to its solutions and stabilities, with consideration of existing theoretical works on the longitudinal stabilities on the solitary-wave solutions to the fifth-order KP equation [8,11].

In 2D, in the weakly nonlinear small-amplitude limit, the fifth-order KP equation is reduced to the integrable nonlinear Schrödinger equation whose solution is stable to longitudinal perturbations (the relevant eigenvalue or the growth rate is purely imaginary). Therefore, one may be tempted to assume that both 2D depression and elevation gravity-capillary solitary-wave solutions to the fifth-order KP equation are stable. However, direct numerical simulations of the fifth-order KP equation reveal that only 2D depression gravity-capillary solitary waves are stable to longitudinal perturbations. 2D

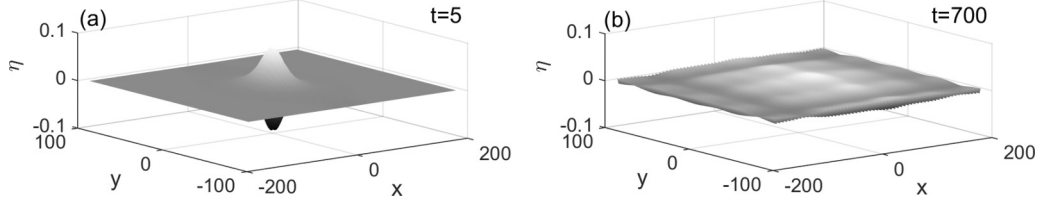

FIG. 13. Evolution of the initially perturbed 3D small-amplitude elevation solitary wave with $c = -1.01$, corresponding to the contraction-type perturbation case (-10%) in Fig. 11(b).

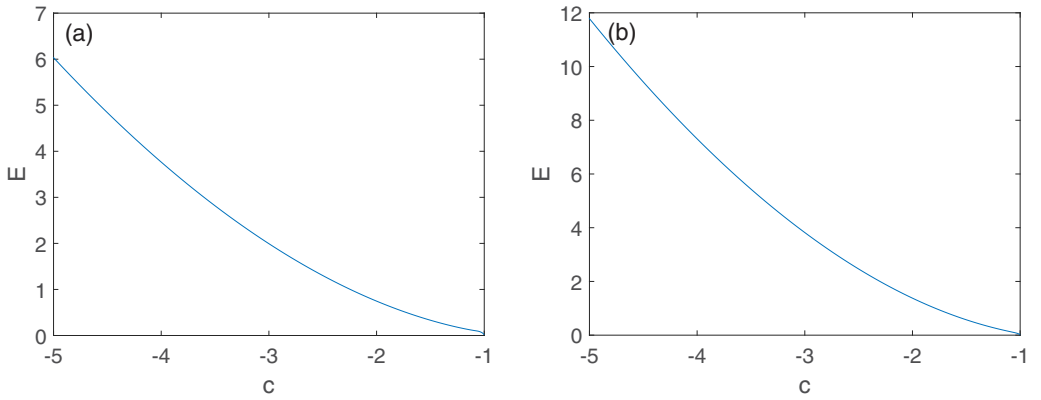

FIG. 14. E-c curves for 2D gravity-capillary solitary waves on shallow water (a) depression waves and (b) elevation waves.

elevation gravity-capillary solitary waves are unstable to longitudinal perturbations and finally evolve into 2D depression gravity-capillary solitary waves. In 3D, in the weakly nonlinear small-amplitude limit, the fifth-order KP equation is reduced to a nonintegrable elliptic-elliptic BRDS equation system whose solution is unstable to a longitudinal perturbation. If the perturbation is a dilation type, the solution blows up to infinity in a finite time. If the perturbation is a contraction type, the solution disperses out to be zero. However, direct numerical simulations of the fifth-order KP equation show more complex results which cannot be predicted by the BRDS equation system. 3D finite-amplitude depression gravity-capillary solitary waves are stable to longitudinal perturbations. 3D finite-amplitude elevation gravity-capillary solitary waves are unstable to longitudinal perturbations and finally evolve into an oscillatory state between two 3D finite-amplitude depression gravity-capillary solitary waves. 3D small-amplitude depression and elevation gravity-capillary solitary waves are unstable to dilation-type longitudinal perturbations and finally evolve into an oscillatory state between two 3D finite-amplitude depression gravity-capillary solitary waves. 3D small-amplitude depression and elevation gravity-capillary solitary waves are unstable to contraction-type longitudinal perturbations and finally become dispersed out toward calm water. All these longitudinal stability results for 3D gravity-capillary solitary waves are related to the existence of an energy minimum which is a necessary condition for a change of stability. Finally, 2D depression and elevation gravity-capillary solitary waves are unstable to transverse perturbations and eventually evolve into 3D finite-amplitude depression gravity-capillary solitary waves. In particular, based on the linear stability analysis, we present a theoretical proof for a long-wave transverse instability of 2D depression and elevation gravity-capillary solitary waves on shallow water. Although the method of the proof may be regarded as standard, its application to the fifth-order KP equation is new. In summary, the only stable ones are 3D finite-amplitude depression gravity-capillary solitary waves.

The present stability results of gravity-capillary solitary waves on shallow water are very similar to those of gravity-capillary solitary waves on deep water, although they have overall different wave profiles; shallow-water gravity-capillary solitary waves are more wrinkled (wave-packet-shaped) than deep-water ones. What is common between shallow-water ($B < 1/3$ and $B \approx 1/3$) and deep-water ($B \approx 0$) gravity-capillary solitary waves is the dispersion relation which features a minimum phase speed at a finite wavelength. The

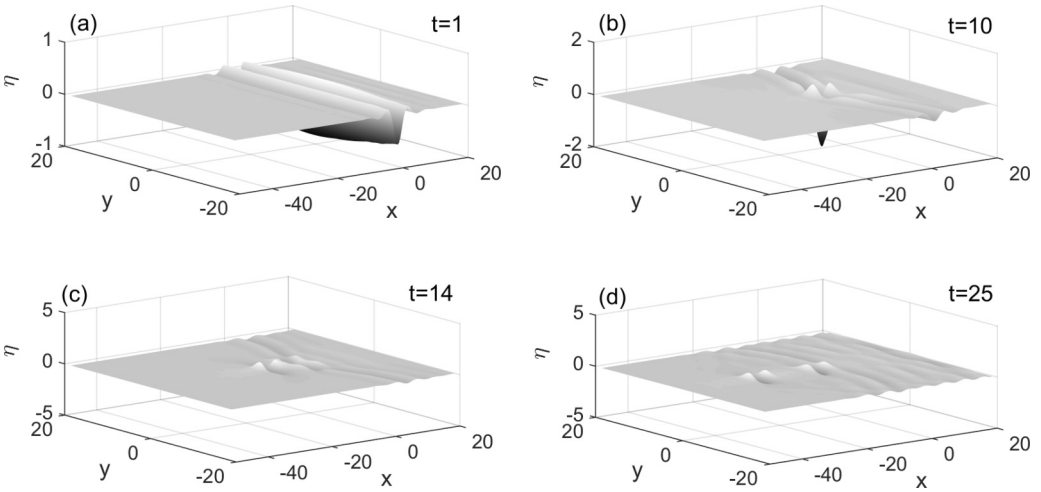

FIG. 15. Transverse instability of a 2D depression gravity-capillary solitary wave $\bar{\eta}(x)$ with a speed $c = -2$ and the resultant formation of 3D depression gravity-capillary solitary waves on shallow water. The initial condition is $\eta(x, y, t = 0) = \bar{\eta}(x) + \bar{\eta}_x \cos(y/12)$.

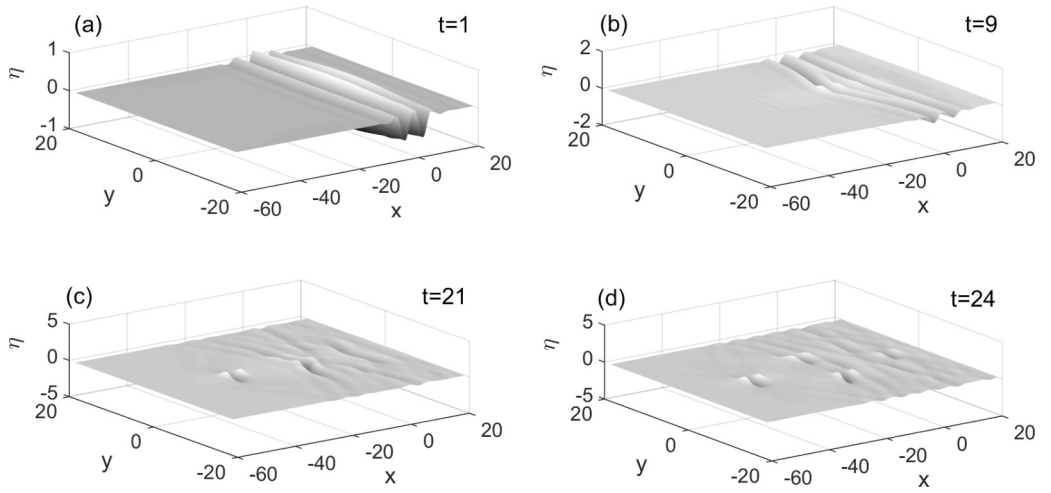

FIG. 16. Transverse instability of a 2D elevation gravity-capillary solitary wave $\bar{\eta}(x)$ with a speed $c = -2$ and the resultant formation of 3D depression gravity-capillary solitary waves on shallow water. The initial condition is $\eta(x, y, t = 0) = \bar{\eta}(x) + \bar{\eta}_x \cos(y/12)$.

minimum phase speed of linear gravity-capillary waves on deep water is 23 cm/s at finite wavelength 1.71 cm. The minimum phase speed of linear gravity-capillary waves on shallow water depends on the Bond number B or the water depth. Therefore, apart from water waves, we may extend the present stability results to other wave systems where the dispersion relation features a minimum at a nonzero wave number or a finite wavelength. One such example is ice waves or flexural-gravity waves on the surface of deep water. In this instance, the flexural rigidity plays a role of the surface tension, thus, the resultant dispersion relation features a minimum at a nonzero wave number [22,23].

ACKNOWLEDGMENT

This work was supported by National Research Foundation of Korea (NRF) under Grant No. NRF-2017R1D1A1B03028299.

APPENDIX: HEURISTIC DERIVATION OF THE FIFTH-ORDER KP EQUATION

The linear dispersion relation of two-dimensional (plane) gravity-capillary waves in water of a finite depth h is as follows.

$$\omega^2 = \left(gk + \frac{Tk^3}{\rho}\right)\tanh kh, \tag{A1}$$

where ω is the angular velocity, g the gravitational acceleration, T the surface tension, ρ the water density, and k the wave number. In a dimensionless form, using h as a length scale and $\sqrt{h/g}$ as a timescale, Eq. (A1) becomes the following dimensionless form.

$$\omega'^2 = (k' + Bk'^3)\tanh k', \tag{A2}$$

where $k' = kh$, $\omega' = \omega/\sqrt{g/h}$, and $B = T/\rho g h^2$(Bond number). Then, dropping primes, the square of the phase speed (c_p^2) is

$$c_p^2 = \frac{\omega^2}{k^2} = \left(\frac{1}{k} + Bk\right)\tanh k, \tag{A3}$$

which features a minimum at $k = 0$ for $B > 1/3$ and at a nonzero wave number $(k \neq 0)$ for $B < 1/3$. For dimensionless wavelengths, $0 < k < \pi/2$, using the following equality.

$$\tanh k = k - \tfrac{1}{3}k^3 + \tfrac{2}{15}k^5 - \tfrac{17}{315}k^7 + \cdots. \tag{A4}$$

Then, Eq. (A2) becomes

$$\begin{aligned}\omega^2 &= (k + Bk^3)\left(k - \frac{1}{3}k^3 + \frac{2}{15}k^5 \cdots\right)\\ &= k^2\left\{1 + \left(B - \frac{1}{3}\right)k^2 + \left(\frac{2}{15} - \frac{B}{3}\right)k^4 + \cdots\right\}.\end{aligned} \tag{A5}$$

Then, the following polynomial relationship between ω and k holds for $B \approx 1/3$ and $0 < k \ll 1$.

$$\begin{aligned}\omega &= k\left\{1 + \left(B - \frac{1}{3}\right)k^2 + \frac{1}{45}k^4 + \cdots\right\}^{1/2}\\ &\approx k\left[1 + \frac{1}{2}\left(B - \frac{1}{3}\right)k^2 + \frac{1}{90}k^4 + \cdots\right].\end{aligned} \tag{A6}$$

Extending to the 3D case by replacing k with κ,

$$\kappa = \sqrt{k^2 + l^2}, \tag{A7}$$

where k is the wave number in one direction (say, x), and l the wave number in the correspondingly transverse direction (say, y). Then, Eq. (A6) becomes

$$\begin{aligned}&\omega - \sqrt{k^2 + l^2} - \tfrac{1}{2}\left(B - \tfrac{1}{3}\right)(k^2 + l^2)^{3/2}\\ &-\tfrac{1}{90}(k^2 + l^2)^{5/2} + \cdots = 0.\end{aligned} \tag{A8}$$

Then, assuming the almost unidirectional wave propagation in x such that

$$\sqrt{k^2+l^2} = k\left(1+\frac{l^2}{k^2}\right)^{1/2} \approx k\left(1+\frac{l^2}{2k^2}\right) = k+\frac{l^2}{2k}, \quad \text{(A9)}$$

Eq. (A8) can be written as follows, taking into account the leading order effect of the transverse variation.

$$\omega - k - \frac{1}{2}\left(B-\frac{1}{3}\right)k^3 - \frac{1}{90}k^5 - \frac{l^2}{2k}\cdots = 0. \quad \text{(A10)}$$

By replacing ω with $-i\partial/\partial t$, k with $i\partial/\partial x$, and l with $i\partial/\partial y$, the following fifth-order linear wave equation in terms of the wave elevation (η) can be derived.

$$\{\eta_t + \eta_x - \tfrac{1}{2}\left(B-\tfrac{1}{3}\right)\eta_{xxx} + \tfrac{1}{90}\eta_{xxxxx}\}_x + \tfrac{1}{2}\eta_{yy} = 0. \quad \text{(A11)}$$

Then, in the moving frame ($x' = x - t$), combined with a KdV-type quadratic nonlinearity and, after dropping primes, the following nonlinear wave equation is obtained.

$$\{\eta_t + \beta(\eta^2)_x - \tfrac{1}{2}\left(B-\tfrac{1}{3}\right)\eta_{xxx} + \tfrac{1}{90}\eta_{xxxxx}\}_x + \tfrac{1}{2}\eta_{yy} = 0. \quad \text{(A12)}$$

By rescaling the above equation using $\eta = a\tilde{\eta}$, $t = b\tilde{t}$, $x = d\tilde{x}$, and $y = e\tilde{y}$, where

$$a = \frac{1}{30\beta}\left[-\frac{2}{(B-1/3)45}\right]^2, \quad \text{(A13a)}$$

$$b = 90\left[-\frac{2}{(B-1/3)45}\right]^{5/2}, \quad \text{(A13b)}$$

$$d = \left[-\frac{2}{(B-1/3)45}\right]^{1/2}, \quad \text{(A13c)}$$

$$e = 3\sqrt{5}\left[-\frac{2}{(B-1/3)45}\right]^{3/2}, \quad \text{(A13d)}$$

and dropping tildes, the following fifth-order KP equation in a normalized form can be obtained.

$$\{\eta_t + 3(\eta^2)_x + 2\eta_{xxx} + \eta_{xxxxx}\}_x + \eta_{yy} = 0. \quad \text{(A14)}$$

Finally, in the frame of reference moving with a speed c ($x' = x - ct$), Eq. (A14) is rewritten as, by dropping primes,

$$\{\eta_t - c\eta_x + 3(\eta^2)_x + 2\eta_{xxx} + \eta_{xxxxx}\}_x + \eta_{yy} = 0. \quad \text{(A15)}$$

[1] B. Kadomtsev and V. Petviashvili, Sov. Phys. Dokl. **15**, 539 (1970).
[2] K. Berger and P. A. Milewski, SIAM J. Appl. Math. **61**, 731 (2000).
[3] P. A. Milewski, Commun. Math. Sci. **3**, 89 (2005).
[4] M. Maleewong, J. Asavanant, and R. Grimshaw, Theor. Comput. Fluid Dyn. **19**, 237 (2005).
[5] E. I. Parau, J.-M. Vanden-Broeck, and M. J. Cooker, Phys. Fluids **17**, 122101 (2005).
[6] M. Maleewong, R. Grimshaw, and J. Asavanant, Eur. J. Mech. B: Fluids **24**, 502 (2005).
[7] E. I. Parau, J.-M. Vanden-Broeck, and M. J. Cooker, J. Fluid Mech. **536**, 99 (2005).
[8] D. C. Calvo, T.-S. Yang, and T. R. Akylas, Proc. R. Soc. London, Ser. A **456**, 469 (2000).
[9] B. Akers and P. A. Milewski, Stud. Appl. Math. **122**, 249 (2009).
[10] P. A. Milewski, J.-M. Vanden-Broeck, and Z. Wang, J. Fluid Mech. **664**, 466 (2010).
[11] T. R. Akylas and Y. Cho, Philos. Trans. R. Soc., A **366**, 2761 (2008).
[12] B. Akers and P. A. Milewski, SIAM J. Appl. Math. **70**, 2390 (2010).
[13] B. Akers and P. A. Milewski, Stud. Appl. Math. **121**, 49 (2008).
[14] B. Kim, J. Eng. Math. **74**, 19 (2012).
[15] Z. Wang and J.-M. Vanden-Broeck, SIAM J. Appl. Math. **75**, 978 (2015).
[16] B. Park and Y. Cho, J. Fluid Mech. **834**, 92 (2018).
[17] B. Kim and T. R. Akylas, J. Eng. Math. **58**, 167 (2007).
[18] L. Paumond, Math. Comput. Simul. **69**, 477 (2005).
[19] Y. Cho, J. Eng. Math. **91**, 37 (2015).
[20] D. J. Benney and G. J. Roskes, Stud. Appl. Math. **48**, 377 (1969).
[21] A. Davey and K. Stewartson, Proc. R. Soc. London, Ser. A **338**, 101 (1974).
[22] R. J. Hosking, A. D. Sneyd, and D. W. Waugh, J. Fluid Mech. **196**, 409 (1988).
[23] R. M. S. M. Schulkes and A. D. Sneyd, J. Fluid Mech. **186**, 25 (1988).